THEORETICAL STUDY OF A CONCENTRIC TUBES EVAPORATOR OF A REFRIGERATION SYSTEM

Maia, Antônio Augusto Torres
Fundação Universidade de Itaúna, Faculdade de Engenharia
Rodovia MG 431 - Km 45 – Campus Verde, 35680-142, Itaúna – Minas Gerais – Brasil.
aamaia@uit.br

Machado, Luiz
Universidade Federal de Minas Gerais, Departamento de Engenharia Mecânica
Av. Antônio Carlos, 6627, Pampulha, 31270-901, Belo Horizonte – Minas Gerais – Brasil.
luizm@demec.ufmg.br

Koury, Ricardo Nicolau Nassar
Universidade Federal de Minas Gerais, Departamento de Engenharia Mecânica
Av. Antônio Carlos, 6627, Pampulha, 31270-901, Belo Horizonte – Minas Gerais – Brasil.
koury@demec.ufmg.br

Abstract. *The experimental study in the refrigeration field is a difficult task. In addition to the generally high costs and the difficulties related with the test bench construction, the tests execution demands effort and time. An alternative that has been employed by many researchers consists in using a mathematical model to simulate the physical system. Compared with the experimental approach, this option offers some advantages, among them it should be emphasized the versatility and the quickness in obtaining results. In this work it is presented a mathematical model for a concentric tubes evaporator. The evaporator was divided into a number of control volumes. A time dependent partial differential equations system was achieved through balances of mass, energy and momentum in each control volume. Correlations obtained from literature were employed to estimate the heat transfer coefficient, pressure drop and void fraction. The theoretical results were compared with experimental data obtained from the refrigerating machine test bench of the DEMEC-UFMG. The good agreement observed validated the proposed mathematical model.*

Keywords*: Concentric tubes evaporator, Mathematical model, Refrigeration system.*

1. Introduction

Mathematical models are being more and more employed in the refrigeration field. Considering that the experimental approach generally requires more effort and time to be developed and it is normally more expensive than the theoretical approach, to make use of a mathematical model can be advantageous to investigate a variety of options and to reduce the number of experiments required in a research work.

In the last decades several works in the refrigeration field were made with the aid of mathematical models. The study of refrigerating fluids non aggressive to the ozone layer (Jung et al., 1991; Domanski et al.,1992 and Sami et al. 1995) and the development of refrigerating machines with improved energetic efficiency (Conde et al.,1991; Sand et al., 1994; Bensafi et al., 1997; Bansal et al., 1999; Tian et al., 2004; Wu et al., 2005 and Maia, 2005) are some examples of mathematical models applications. In both cases, the experimental approach would require the replacement of many parts of the refrigeration circuit. Using a mathematical model many situations can be simulated demanding for it just the modified parts characteristics, that could be provided to the computational program through a data file. Even if exists a test bench available, the theoretical results can be useful if used to plan the experimental tests and to introduce same modifications in the experimental apparatus. This procedure can eliminate the less promising alternatives in advance and reduce significantly the number of experiments needed in a research.

In this work is presented a mathematical model to simulate the dynamic behavior of a concentric tubes evaporator. This model is based on the prototype project and built in the Mechanical Department of the Federal University of Minas Gerais.

2. Experimental apparatus

The experimental device used is shown in Fig. (1). This device consists of a vapor compression refrigerating system, which has R134a as the refrigeration fluid and, as secondary fluid, pure water in the evaporator and in the condenser. The system is basically composed by a reciprocating compressor, a condenser, a sub-cooler, an evaporator, three expansion valves and systems to do measures and data acquisition. The compressor is alternative type and it has a piston displacement of 157 cm^3. A three-phase electrical motor is employed to drive the compressor. This electrical motor is powered by a frequency inverter that enables the variation of the revolution speed of the motor-compressor assemblage in a range of 0 to 300 Hz. The condenser is shell and tube type and it has a 6 kW capacity. The temperature of the secondary fluid in the condenser is adjusted by mixing warm water that comes from the condenser itself with

room temperature water, coming from the feeding system. The sub-cooler is coaxial type, made of an envelope tube and of an internal tube in "U". The evaporator is a multiple tube coaxial type and it is composed by an envelope tube of PVC and of three inner cooper tubes through which flows the refrigeration fluid. Water flows in counter flow in the annular space between the PVC and cooper tubes. The evaporator was projected to provide a maximum refrigeration capacity of 3 kW. The set of tubes was assembled so that the evaporator becomes more compact and, at the same time, promotes a greater turbulence in the flow of the fluids. In the evaporator, the secondary fluid temperature is maintained within the desired limits by an electrical heating system. The experimental bench has three expansion valves placed in parallel (manual, thermostatic and electronic type). A blockage valve permits the isolated operation of each expansion device. In this work, only a manual expansion valve was used. Eleven T type thermocouples (cooper-constantan) were used to measure temperature. They were implanted inside the tubes at the inlet and outlet of each system component.

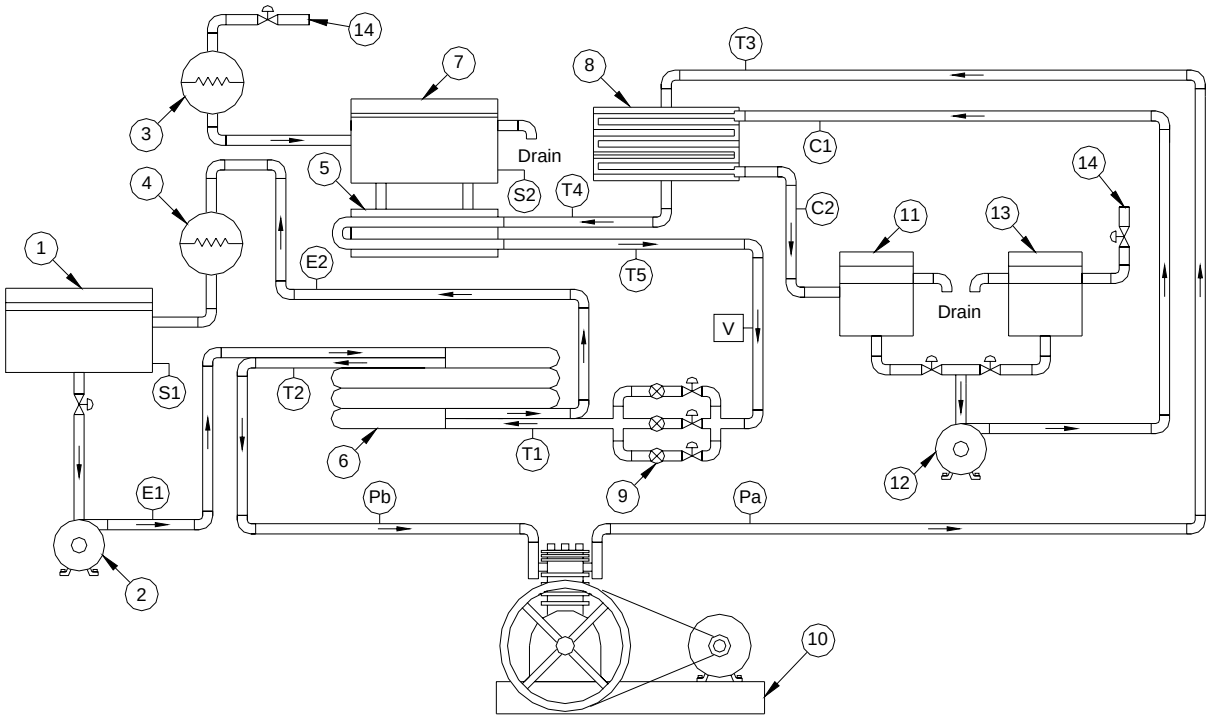

Figure 1 – Schematic configuration of the experimental bench

Legend:

1. Water reservoir (evaporator)
2. Water pump (evaporator)
3. Electric heater (sub-cooling)
4. Electric heater (evaporator)
5. Cooler
6. Evaporator
7. Water reservoir (sub-cooling)
8. Condenser
9. Expansion devices
10. Reciprocating compressor
11. Hot water reservoir (condenser)
12. Water pump (condenser)
13. Cold water reservoir (condenser)
14. Water feed

V. Flow meter
Pa. Pressure sensor (condensation)
Pb. Pressure sensor (evaporation)
S1,S2. Temperature sensor (PID)
T1-T5. Temperature sensor of the refrigeration fluid
E1,E2. Temp.sensor (water at inlet and outlet of the evaporator)
C1,C2. Temp. sensor (water at inlet and outlet of the condenser)

Two piezoresistive pressure sensors were installed at the inlet and outlet of the expansion devices. At the entrance the sensor has a range of measurement from 0 to 2.4 MPa, while at the exit the range is from 0.1 to 0.9 MPa. Both sensors have an uncertainty of $\pm$ 0.2%. A differential pressure sensor permits to measure the pressure drop of the refrigeration fluid at the heat exchangers (evaporator and the condenser). Its range of measurement is from 0 to 0.25 MPa, with uncertainty of $\pm$ 0.075%. The refrigerant mass flow was measured with a Coriolis flow meter. Its range of measurement is from 15 to 200 kg/h. A software provided with the flow meter computes the maximum uncertainty of this instrument based on the measured mass flow. To determine the mass flow of the secondary fluid in the evaporator, a test tube (with subdivisions of 20 ml) and a digital chronometer were used. All the signals generated by the different sensors of the test bench are received and treated by a data acquisition system in real time.

3. Mathematical model

The mathematical model proposed in this work consists on the model of two components treated separately. In addition to the evaporator model it is also necessary the compressor model to estimate the mass flow rate at the outlet of this component. The mass flow rate estimated by both, the compressor and the evaporator model, are needed to be compared with each other at every time instant and used as one of the convergence criteria.

3.1. Compressor model

Some alternative type compressor models found in the literature are very complex, considering time and space discretization**.** This strategy generally permits a more accurate estimative of the pressure drop in the valves, the mass flow rate and the heat transfer coefficients. The compressor model developed in this work is very simple. On its implementation it was not considered: (1) Pressure drop in the valves; (2) Mass flow rate variation at the inlet and outlet; (3) The compressor thermal inertia. Along with these considerations it is assumed that: (4) The compression process is adiabatic.

In the compressor model, the input variables are the evaporation pressure (P_{f2}), the condensation pressure (P_{f3}) and the superheating degree (ΔT_s). The output variable is the mass flow rate at the outlet of the compressor ($\dot{m}_{f3}$). The mass flow rate estimative was done using the following expression:

$$\dot{m}_{f3} = N \cdot V \cdot \rho_{f2} \cdot \eta_v \tag{1}$$

where $\dot{m}_{f3}$, N, V, ρ_{f2} and η_v are respectively the mass flow rate, the rotational speed, the piston displacement volume, the specific mass at the compressor inlet and the volumetric efficiency. The volumetric efficiency can be estimated by the following equation:

$$\eta_v = 1 + c - c \cdot \left(\frac{P_{f3}}{P_{f2}} \right)^{\frac{1}{n}} \tag{2}$$

where c is the clearance ratio determined experimentally, P_{f3} and P_{f2} represent the condensing and evaporation refrigerant pressures. Once the compression process was considered adiabatic, n represents the quotient between the constant pressure and constant volume specific heats.

3.2. Evaporator model

In order to develop the evaporator model, the following simplifications were considered: (1) The refrigerant liquid and vapor phases are in thermodynamic equilibrium; (2) The axial heat transfer was neglected; (3) The evaporator has a perfect thermal insulation; (4) The physical properties related with refrigerant, secondary fluid and pipe wall were considered uniform in the evaporator cross section; (5) The refrigerant and secondary fluid potential energy was not taken into account.

In the evaporator model, the input variables are the refrigerant mass inside the evaporator (M), the mass flow rate ($\dot{m}_{f1}$) and the refrigerant enthalpy (h_{f1}) at the inlet of the evaporator, the secondary fluid mass flow rate ($\dot{m}_a$), the secondary fluid temperature (t_{a1}) at the inlet of the evaporator. The output variables are the refrigerant temperature at the inlet and outlet of the evaporator, the secondary fluid temperature at the outlet of the evaporator and various spatial patterns like pressure, enthalpy, temperature, etc.. The evaporator model was established by dividing this component in to a number of control volumes and applying the principles of energy conservation (refrigerant, secondary fluid and pipes wall), as well as mass and momentum conservation (refrigerant). This procedure generates the following set of differential equations:

Refrigerant fluid (energy, mass and momentum conservation):

$$A_f \cdot \frac{\partial}{\partial t}\left[\rho_f \cdot (h_f - P_f \cdot v_f)\right] = -A_f \cdot \frac{\partial}{\partial z}(G_f \cdot h_f) + \alpha_f \cdot p_f \cdot (T_p - T_f) \tag{3}$$

$$\frac{\partial \rho_f}{\partial t} + \frac{\partial G_f}{\partial z} = 0 \tag{4}$$

$$\frac{\partial}{\partial z}\left\{P_f + G_f^2 \cdot \left[\frac{x^2 \cdot \nu_v}{\alpha} + \frac{(1-x)^2 \cdot \nu_l}{1-\alpha}\right]\right\} = -\frac{\partial G_f}{\partial t} - \left(\frac{dP}{dz}\right)_F - g \cdot \rho_f \cdot sin(\theta) \tag{5}$$

Secondary fluid (energy conservation):

$$\rho_a \cdot A_a \cdot c_{pa} \cdot \frac{\partial T_a}{\partial t} = -G_a \cdot A_a \cdot c_{pa} \cdot \frac{\partial T_a}{\partial z} - \alpha_a \cdot p_a \cdot (T_a - T_p) \tag{6}$$

$$\rho_p \cdot A_p \cdot c_{pp} \cdot \frac{\partial T_p}{\partial t} = \alpha_a \cdot p_a \cdot (T_a - T_p) - \alpha_f \cdot n \cdot p_f \cdot (T_p - T_f) \tag{7}$$

The subscripts f, p, a, l and v are related with refrigerant fluid, tube wall, secondary fluid, liquid and vapor phases, respectively. The variables A, G, h, T, P, p, x, ν, g, ρ, n and θ are the cross section area, the mass flux, the enthalpy, the temperature, the pressure, the wet perimeter, the vapor quality, the specific volume, the gravity acceleration, the specific mass, the number of tubes and the pipe inclination. The variable α when indexed represents the heat transfer coefficient and when it is not indexed it represents the void fraction. The mass flux can be estimated by the quotient between the mass flow rate and the cross section passage area. The refrigerant specific mass was computed using the following equation, where ρ_l and ρ_v are the liquid and vapor specific mass.

$$\rho = \rho_l + \alpha \cdot (\rho_v - \rho_l) \tag{8}$$

The correlations utilized in this work to estimate the heat transfer coefficient, the void fraction, and the pressure drop due the friction were obtained from the technical literature. To estimate the evaporation heat transfer coefficient, at first the evaporator was divided in three regions: evaporation region, liquid deficient region and superheating region. The quality and the critical quality ($x_{critical}$) were used as parameters to determine the start point and the end point of each region. The critical quality can be estimated through the correlation proposed by Sthapak (Maia, 2005):

$$x_{critical} = 7{,}943 \cdot \left[Re_v \cdot \left(2{,}03 \cdot 10^4 \cdot Re_v^{-0,8} \cdot (T_p - T_{sat}) - 1\right)\right]^{-0,161} \tag{9}$$

where Re, T_p and T_{sat} are the number of Reynolds, the wall tube temperature and the saturation temperature. Once defined the critical quality, the evaporation region was supposed to be settled while $x < x_{crittical}$,; the liquid deficient region was assumed to occur from $x = x_{critical}$ to $x = 1$ and the superheating region occurs when $x > 1$. For the evaporation region, the evaporation heat transfer coefficient (α_{eb}) was estimated using the correlation proposed by Dengler and Addoms (Maia, 2005). For the liquid deficient region (α_{def}), the heat transfer coefficient was estimated using a third order polynomial as presented bellow.

$$\alpha_{def} = a_0 + a_1 \cdot x + a_2 \cdot x^2 + a_3 \cdot x^3 \tag{10}$$

where x represents the quality. For the superheating region (α_v), the heat transfer coefficient was estimated using the correlation proposed by Dittus-Boelter (Maia, 2005). To determine the coefficients (a_i) presented in the Eq. (10) it is needed four mathematical relations. These relations are:

$$\alpha_{def}(1) = \alpha_v(1) = a_0 + a_1 + a_2 + a_3 \tag{11}$$

$$\alpha_{def}(x_{critical}) = \alpha_{eb}(x_{critical}) = a_0 + a_1 \cdot x_{critical} + a_2 \cdot x_{critical}^2 + a_3 \cdot x_{critical}^3 \tag{12}$$

$$\left[\frac{\partial \alpha_{def}}{\partial x}\right]_{x=1} = \left[\frac{\partial \alpha_{def}}{\partial z} \cdot \frac{\partial z}{\partial x}\right]_{x=1} = a_1 + 2 \cdot a_2 + 3 \cdot a_3 = 0 \tag{13}$$

$$\left[\frac{\partial \alpha_{def}}{\partial x}\right]_{x=x_{critical}} = \left[\frac{\partial \alpha_{eb}}{\partial x}\right]_{x=x_{critical}} = \left[\frac{\partial \alpha_{eb}}{\partial z} \cdot \frac{\partial z}{\partial x}\right]_{x=x_{critical}} = a_1 + 2 \cdot a_2 \cdot x_{critical} + 3 \cdot a_3 \cdot x_{critical}^2 \tag{14}$$

In the Eq. (13) and (14), the variable z represents the position axis.

The void fraction was estimated using the correlation proposed by Hughmark. The pressure drop along the tubes for the two phase flow was compute by the Lockhart-Martinelli correlation and, for the single phase flow, it was used the correlation proposed by Fanning. Details about all correlations employed in this work can be found in Maia (2005).

The simultaneous solution of the Eq. (3) to (7) is very complicated due the fact that the refrigerant flow and the water flow are in opposite directions. To overcome this problem the Eq. (3) to (5) were solved separately using the fourth order Runge-Kutta method, along the z axis. To obtain enthalpy gradient in the z direction, the Eq. (3) and (4) were combined resulting in:

$$\frac{\partial h_f}{\partial z} = \frac{1}{G_f}\left[\frac{\partial P_f}{\partial t} - \rho_f \cdot \frac{\partial h_f}{\partial t} + \frac{\alpha_f \cdot p_f}{A_f} \cdot (T_p - T_f)\right] \tag{15}$$

The mass flux gradient can be calculated by the following expression:

$$\frac{\partial G_f}{\partial z} = -\frac{\partial \rho_f}{\partial t} \tag{16}$$

To calculate the pressure gradient in the z direction it was necessary to define a modified pressure given by:

$$\overline{P}_f = P_f + G_f^2 \cdot \left[\frac{x^2 \cdot v_v}{\alpha} + \frac{(1-x)^2 \cdot v_l}{1-\alpha}\right] \tag{17}$$

From the Eq. (17), the Eq. (5) can be written as:

$$\frac{\partial \overline{P}_f}{\partial z} = -\frac{\partial G_f}{\partial t} - \left(\frac{dP}{dz}\right)_F + g \cdot \rho_f \cdot sin(\theta) \tag{18}$$

Now the modified pressure can be determined using the Runge-Kutta method. The result obtained should be used in the Eq. (17) to determine the pressure gradient in the z direction. Before applying the Runge-Kutta method in the Eq. (18), the time dependent derivative was determined from the following expression:

$$\frac{\partial G_f}{\partial t} = \frac{G_f - G_f^0}{\Delta t} \tag{19}$$

where Δt is the time step and the superscript "0" refers to the values of G_f taken at t-Δt instant. In an analogous way, this procedure was utilized to calculate the time dependent derivatives in the Eq. (15) and (16).

The solution of the Eq. (6) and (7) was performed using the finite difference implicit method. In this way, the continuous physical domain was discretized and the exact derivatives were replaced by finite difference approximations. This procedure generated an algebraic finite difference approximation of the differential equations, as presented below:

$$\rho_p \cdot A_p \cdot c_{pp} \cdot \frac{T_p(i) - T_p(i)^0}{\Delta t} = \alpha_a \cdot p_a \cdot (T_a - T_p) - \alpha_f \cdot n \cdot p_f \cdot (T_p - T_f) \tag{20}$$

$$\rho_a \cdot A_a \cdot c_{pa} \cdot \frac{T_a(i) - T_a(i)^0}{\Delta t} = -G_a \cdot A_a \cdot c_{pa} \cdot \frac{T_a(j-1) - T_a(j)}{\Delta z} - \alpha_a \cdot p_a \cdot (T_a - T_p) \tag{21}$$

Where the i index refers to the center of the control volume and the j index refers to the boundary. To determine the water temperature at the outlet of each element, the following approximation was utilized:

$$T_a(j+1) = 2 \cdot T_a(i) - T_a(j) \tag{22}$$

4. Model validation

4.1 – Steady-state validation

To perform the steady-state model validation, the experimental data were compared with the theoretical results obtained through computer simulations. The values of the input variables as refrigerant mass flow rate, secondary fluid temperature at the inlet of the evaporator, secondary fluid mass flow rate, condensing temperature and sub-cooling

temperature, etc., were obtained from experimental measurements and provided to the mathematical model through a data file. The theoretical steady-state start point was obtained using a very high step time (10^7s).

In the Fig. (2) and (3) is presented a comparison between the experimental and theoretical refrigerant temperatures at the inlet and the outlet of the evaporator. At the inlet of the evaporator, the theoretical temperature showed an average deviation of 0.5ºC. All of the numerical values are between the uncertainty limits of the experimental results. At the out let of the evaporator, the theoretical temperature showed an average deviation of 1.5ºC and half of the numerical values are between the uncertainty limits of the experimental results. The deviations observed in the Fig. (2) and (3) can be due to an inaccurate estimative of the refrigerant mass inside the evaporator. Another reason that also influenced these results is the imprecise evaluation of the heat transfer coefficient in the evaporation region. This region extends through the most part of the evaporator and its heat transfer coefficient is the higher one.

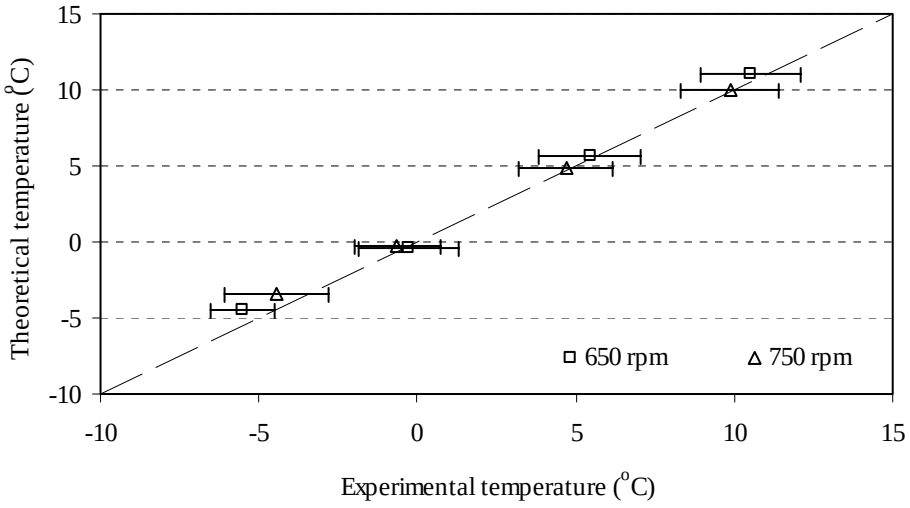

Figure 2 - Comparison between the experimental and theoretical refrigerant temperatures at the inlet of the evaporator

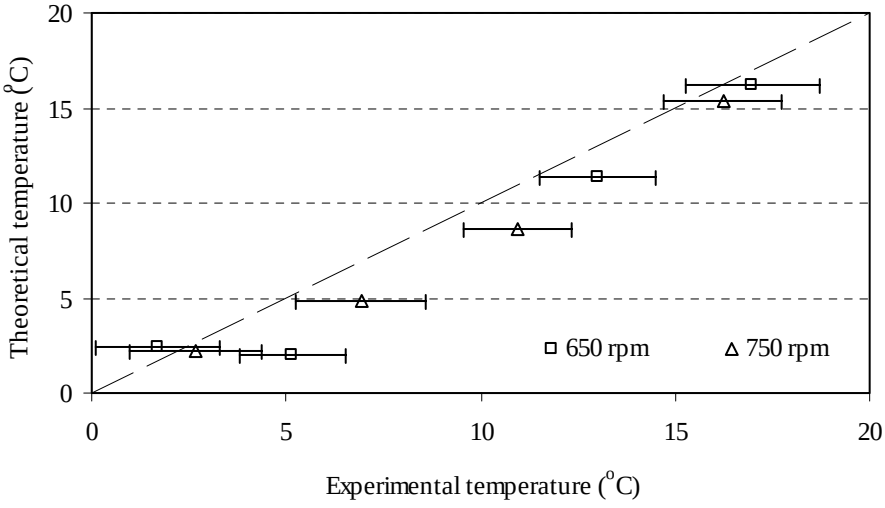

Figure 3 - Comparison between the experimental and theoretical refrigerant temperatures at the outlet of the evaporator

In the Fig. (4) is presented a comparison between experimental and theoretical secondary fluid temperature at the outlet of the evaporator. The agreement observed is very good, showing an average deviation of 0.2ºC. All numerical values are between the uncertainty limits of the experimental data. This good agreement was already expected. The water temperature at the outlet of the evaporator depends basically of the refrigerating capacity. Additionally, the refrigerating capacity depends mainly to the mass flow rate, which was provided as an input variable during the process of model validation.

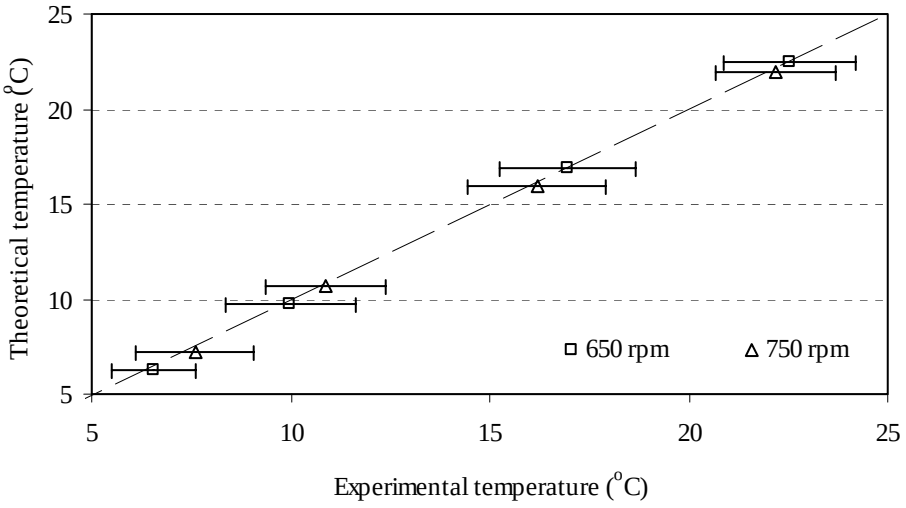

Figure 4 – Comparison between the experimental and theoretical secondary fluid temperatures at the outlet of the evaporator.

4.2 – Transient validation

The procedure of the transient model validation consisted in firstly to obtain the theoretical steady-state start point. This point was obtained using the same strategy mentioned in the steady-state validation. After this, the mass flow rate at the inlet of the evaporator was quickly reduced in 5%. The response generated by the mathematical model was compared with the experimental data obtained in an equivalent way.

In the Fig. (5) is presented the theoretical and experimental response to a step perturbation in the mass flow rate at the inlet of the evaporator. In this figure is being analyzed the refrigerant temperature at the inlet (T_{f1}) and outlet (T_{f2}) of the evaporator. These data were obtained in transient state, with the evaporation temperature in approximately 10ºC and compressor speed at 750 rpm.

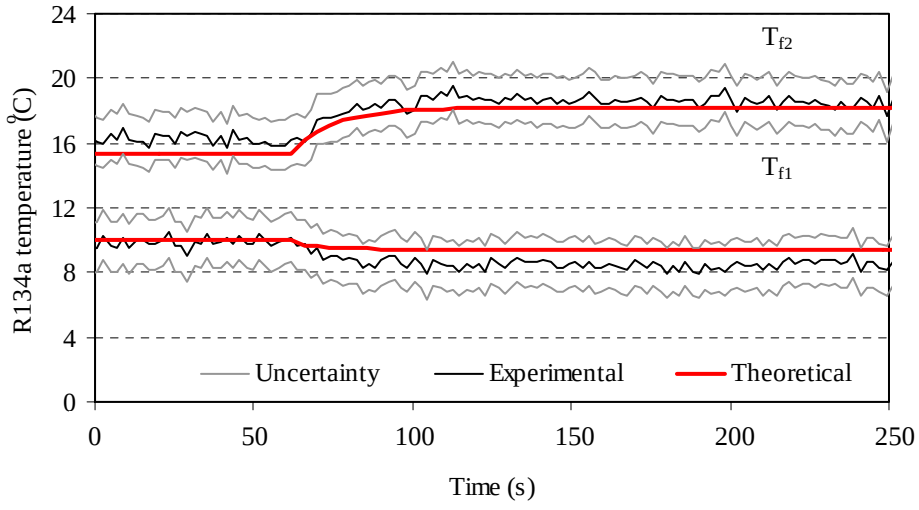

Figure 5 – Theoretical and experimental response of the refrigerant temperature in response to a step perturbation in the mass flow rate at the inlet of the evaporator ($T_{evaporation}$=10ºC and N=750 rpm).

Comparing the results presented in the Fig.(5) it can be noticed that theoretical data are between the uncertainty limits of the experimental results.

In the Fig.(6) is showed a comparison between the theoretical and experimental water temperature at the outlet of the evaporator. It was expected that with the refrigerant mass flow rate reduction and the consequent refrigerating capacity diminution, an increase in the water temperature. Nevertheless, once this variation was small, it was not possible verify this occurrence in the experimental data. In the theoretical data this slight variation can be seen.

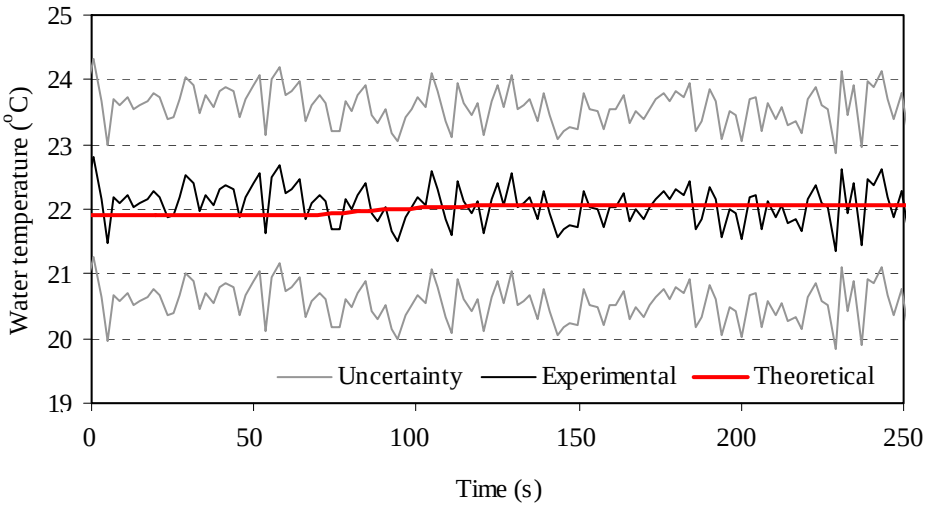

Figure 6 – Theoretical and experimental response of the water temperature at the outlet of the evaporator ($T_{evaporation}$=10ºC and N=750 rpm).

5. – Conclusions

In this work it was presented a mathematical model to simulate the transient behavior of a concentric tubes evaporator. The good agreement observed during the validation process showed that the proposed mathematical model and the numerical methodology utilized were effective in solving the problem. The results obtained can be improved utilizing a more accurate correlation to estimate the heat transfer coefficient in the evaporation region. The model precision can also be enhanced providing a more exact value of the refrigerant mass inside the evaporator in the start of the simulation.

6. References

Bensafi, A, Borg, S. and Parent, D. , 1997, "CYRANO: a computational model for the detailed design of plate-fin-and-tube heat exchangers using pure and mixed refrigerants", International Journal of Refrigeration, Vol. 20, pp. 218-228.

Conde, M. R. and Suter, P., 1991, "A computer program for simulation of domestic heat pumps", XVIII Cong. Int. Refrig., Montreal, pp. 1448-1453.

Domanski, P. A. and McLinden, M. O., 1992, "A simplified cycle simulation model for the performance rating of refrigerants and refrigerants mixtures", Rev. Int. Froid, Vol. 15, nº 2.

Jung, D. S. and Radermacher, R., 1991, "Performance simulation of single-evaporator domestic refrigerators charged with pure and mixed refrigerants", Rev. Int. Froid, Vol. 14, pp. 223-232.

Maia, Antônio A. T., 2005, "Metodologia de desenvolvimento de um algoritmo para controle simultâneo da capacidade de refrigeração e do grau de superaquecimento de um sistema de refrigeração", Tese (Doutorado), Departamento de Engenharia Mecânica, Universidade Federal de Minas Gerais, Belo Horizonte, 160 pp.

Sami, S. M. and Zhou, Y., 1995, "Numerical prediction of heat pump dynamic behavior using ternary non-azeotropic refrigerant mixtures", International Journal of Energy Research, Vol. 19, pp. 19-35.

Sand, J. R., Vineyard, P. E. and Bohman, R. H., 1994, "Investigation of design options for improving the energy efficiency of conventionally designed refrigerator-freezers", ASHRAE Transactions, v. 100, part 1, pp.1359-1368.

Tian, C., Dou, C., Yang, X. and Li, X. , 2004, "A mathematical model of variable displacement wobble plate compressor for automotive air conditioning system", Applied Thermal Engineering, v. 24, pp. 2467-2486.

Wu, C., Xingxi, Z. and Shiming, D., 2005, "Development of control method and dynamic model for multi-evaporator air conditioners (MEAC)", Energy Conversion & Management, v. 46, pp. 451-465.

7. Responsibility notice

The authors are the only responsible for the printed material included in this paper.